Behavioral/Cognitive

Time Persistence of the FMRI Resting-State Functional Brain Networks

Shu Guo,[1,2] Orr Levy,[3,4] Hila Dvir,[2] Rui Kang,[5,6] Daqing Li,[5,7] Shlomo Havlin,[2*] and Vadim Axelrod[8*]

[1]State Key Laboratory of Cognitive Neuroscience and Learning, Beijing Normal University, Beijing 100875, China, [2]Department of Physics, Bar-Ilan University, Ramat Gan 52900, Israel, [3]Department of Immunobiology, Yale University School of Medicine, New Haven, Connecticut 06520-8011, [4]Howard Hughes Medical Institute, Chevy Chase, Maryland 20815, [5]School of Reliability and Systems Engineering, Beihang University, Beijing 100191, China, [6]Yunnan Innovation Institute, Beihang University, Kunming 650233, China, [7]College of Safety Science and Engineering, Civil Aviation University of China, Tianjin 300300, China, and [8]The Gonda Multidisciplinary Brain Research Center, Bar Ilan University, Ramat Gan 52900, Israel

Time persistence is a fundamental property of many complex physical and biological systems; thus understanding the phenomenon in the brain is of high importance. Time persistence has been explored at the level of stand-alone neural time-series, but since the brain functions as an interconnected network, it is essential to examine time persistence at the network level. Changes in resting-state networks have been previously investigated using both dynamic (i.e., examining connectivity states) and static functional connectivity (i.e., test–retest reliability), but no systematic investigation of the time persistence as a network was conducted, particularly across different timescales (i.e., seconds, minutes, dozens of seconds, days) and different brain subnetworks. Additionally, individual differences in network time persistence have not been explored. Here, we devised a new framework to estimate network time persistence at both the link (i.e., connection) and node levels. In a comprehensive series analysis of three functional MRI resting-state datasets including both sexes, we established that (1) the resting-state functional brain network becomes gradually less similar to itself for the gaps up to 23 min within the run and even less similar for the gap between the days; (2) network time persistence varies across functional networks, while the sensory networks are more persistent than nonsensory networks; (3) participants show stable individual characteristic persistence, which has a genetic component; and (4) individual characteristic persistence could be linked to behavioral performance. Overall, our detailed characterization of network time persistence sheds light on the potential role of time persistence in brain functioning and cognition.

Key words: **fMRI; functional connectivity; individual differences; network persistence; resting-state networks; time persistence**

Significance Statement

Time persistence—how long the system stays in a certain configuration—is a fundamental characteristic property of a variety of complex physical and biological systems. To date, the network time persistence of the brain is not sufficiently well understood. Here, we introduce and test a novel framework to quantify brain network time persistence. We found that the functional brain network becomes gradually less similar within the run (up to 23 min) and even less similar between days. The participants showed stable individual characteristic persistence, which has a genetic component. In addition, individual characteristic persistence could be linked to behavioral performance. Thus, brain network time persistence may play a key role in brain functioning and human cognition.

Received Aug. 19, 2024; revised Nov. 27, 2024; accepted Jan. 22, 2025.

Author contributions: S.G., O.L., D.L., R.K., S.H., and V.A. designed research; S.G., O.L., S.H., and V.A. performed research; S.G., O.L., H.D., and S.H. contributed unpublished reagents/analytic tools; S.G., O.L., and V.A. analyzed data; S.G., O.L., H.D., S.H., and V.A. wrote the paper.

Data were provided in part by the Human Connectome Project, WU-Minn Consortium (Principal Investigators, David Van Essen and Kamil Ugurbil; 1U54MH091657) funded by the 16 National Institutes of Health (NIH) Institutes and Centers that support the NIH Blueprint for Neuroscience Research, and the McDonnell Center for Systems Neuroscience at Washington University. S.G. is supported by the Postdoctoral Fellowship Program (Grade C) of China Postdoctoral Science Foundation under Grant Number GZC20230267. S.H. thanks the support of Israel Ministry of Innovation, Science & Technology (Grant Number 01017980), the Israel Science Foundation (Grant Number 2830/23), the Binational Israel–China Science Foundation (Grant Number 3132/19), and the European Union under the Horizon Europe Grant OMINO (Grant Number 101086321); D.L. thanks the support of the National Natural Science Foundation of China (Grant Number 72225012); V.A. is supported by Israel Science Foundation (Grant Number 342/21); and S.G. thanks Dr. Adrian Kaho Chan for his initial help on this study.

*S.H. and V.A. have equal senior authorship.

The authors declare no competing financial interests.

Correspondence should be addressed to Vadim Axelrod at vadim.axelrod@gmail.com or Daqing Li at daqingl@buaa.edu.cn.

https://doi.org/10.1523/JNEUROSCI.1570-24.2025

Introduction

Time persistence—how long the system stays in a certain configuration (Salcedo-Sanz et al., 2022)—is a characteristic property of a variety of complex systems, such as weather and climate dynamics (Koscielny-Bunde et al., 1998; Wu et al., 2024), evolution (Donges et al., 2011), and economic systems (Hommes, 2021; Wu et al., 2024). The brain is a complex system (Bassett and Gazzaniga, 2011); it is essential therefore to understand persistence properties of the brain. Time persistence (or long-range temporal correlations) of neural signals [e.g., resting-state functional MRI (fMRI) time-courses from regions of interest (ROIs)] has been explored using a variety of recording/imaging methods [e.g., fMRI, electroencephalogram (EEG) and magnetoencephalography (MEG)] at the level of stand-alone time-series (Linkenkaer-Hansen et al., 2001; Palva et al., 2013). Using methods like detrended fluctuation analysis (DFA; Peng et al., 1994) or Hurst exponent (Hurst, 1951) studies revealed that neural time-series exhibit some level of time persistence: using fMRI (He, 2011), using EEG (Palva et al., 2013), and using MEG (Linkenkaer-Hansen et al., 2001). However, note that, even if the system is persistent at the level of stand-alone time-series, that does not imply that it will also be persistent at the network level. For example, in a system in which node signals are sine waves with random phases, the signals at the node level will be persistent, but the system at the network level will not be persistent. Critically, as it is widely accepted that the brain functions as a complex interconnected network (Sporns et al., 2004; Arenas et al., 2008; Bassett and Bullmore, 2009; Markov et al., 2013; Barabási et al., 2023), understanding brain persistence at the network level is more than pertinent.

Changes in brain network connectivity have been widely investigated using the so-called fMRI resting-state functional dynamic connectivity approach, in which connectivity is calculated over a relatively short time window of ∼30–60 s (Hutchison et al., 2013). Brain networks exhibit different interchangeable states, with the appearance of these states lasting for several dozen seconds (Allen et al., 2014; Barttfeld et al., 2015; Abrol et al., 2017; Vidaurre et al., 2017). The transitions between states happen with some probabilities (Allen et al., 2014; Shappell et al., 2019; Jun et al., 2022) and order (Vidaurre et al., 2017; Ma and Zhang, 2018). While these results are undoubtedly important, studies examining dynamic connectivity states have not directly addressed the question of the time persistence of the network as a whole and, in particular, how network similarity changes over intervals longer than several dozen seconds. It is also noteworthy that the dynamic functional connectivity method is not without controversy (e.g., sampling variability; Laumann et al., 2017), thus complicating the interpretation of the results (Lurie et al., 2019; Laumann et al., 2024). In addition to "dynamic," changes in so-called "static" functional connectivity (i.e., runs of 5–10 min duration) have been also examined primarily by studies that looked into the test–retest reliability of functional connectivity across two runs (Zuo and Xing, 2014; Termenon et al., 2016; Gratton et al., 2018; Noble et al., 2019). Their results were not unequivocal, ranging from relatively poor test–retest reliability in recent meta-analysis (Noble et al., 2019) to relatively high functional network stability in a study with long scans of highly sampled individuals (Gratton et al., 2018). Notably, comparison of network changes between only two runs (i.e., two time points), as was the case in most previous test–retest studies, is not equivalent to systematic examination of brain network changes across time.

Overall, despite substantial progress in understanding functional networks, there is still no extant systematic exploration of network time persistence. The specific major unanswered question is to what extent the brain network topology is time persistent across different timescales (i.e., seconds, minutes, dozens of seconds, or days). For example, how much is the network similar to that in the initial time point? Does the similarity reaches its minimum at a certain time point within a run (e.g., a time gap of 5 min), or does the similarity continue to decrease instead? An additional important unexplored aspect is whether there are individual differences in network time persistence and, if so, (1) whether individual differences in network time persistence can be explained by heredity and (2) whether individual network time persistence can be associated with behavioral performance. To address this gap in knowledge, we devised new analytical framework of network time persistence at both the link (i.e., connection) and node levels. Using three resting-state datasets, we applied this framework to systematically investigate network time persistence.

Materials and Methods

Datasets. Our main analysis dataset was the Human Connectome Project Young Adult (HCP-YA) dataset (Van Essen et al., 2012). To examine network time persistence over a longer run duration (30 min), we used the Midnight Scan Club (MSC) dataset (Gordon et al., 2017). For replication, we used the Human Connectome Project in Development (HCP-D) dataset (Harms et al., 2018).

The HCP-YA resting-state dataset was acquired using a 3 T Connectome Skyra Siemens scanner. The full details of the fMRI acquisition protocol have been provided previously (Van Essen et al., 2012; Glasser et al., 2013), so here we only briefly describe the key parameters. The scanning parameters were as follows: TR = 0.72 s; 2.0 mm isotropic voxels; number of volumes per run, 1,200; and run duration, 14.4 min. Participants underwent two resting-state runs per day, and most of the participants were scanned twice on 2 different days. The interval between scanning days varied from 1 d (for most of the participants) to several days; the interval information for each participant was not provided by the HCP consortium. Only participants who underwent scanning on both days were included in the analysis. After excluding 20 participants due to excessive motion in the scanner (see "Data analysis" below), our dataset included 974 participants. From this dataset, we randomly chose 20 participants to estimate independently the $W_{\text{threshold}}$ parameter (see below). The data of the remaining 954 participants [age mean, 28.68 years; age standard deviation (SD), 3.69 years; 519 females] were used in our main analyses. The sample size of ∼1,000 HCP-YA participants has been previously widely used to explore brain functional connectivity and its properties (Siegel et al., 2017; Bijsterbosch et al., 2018; Schaefer et al., 2018; Li et al., 2019). In addition to the fMRI imaging data, the HCP-YA dataset includes the participants' behavioral measures acquired both within and outside the scanner.

The MSC resting-state dataset used to examine network time persistence over a longer run duration was scanned using a 3 T Trio Siemens scanner. The dataset includes 10 healthy, right-handed young adult subjects (five females aged 24–34 years). The full details of the fMRI acquisition protocol have been provided in the original publication (Gordon et al., 2017). Here we briefly describe the key parameters: TR, 2.2 s; 4.0 mm isotropic voxels; and number of volumes per run, 818. Each participant was scanned 10 times on 10 subsequent days. The duration of each run was 30 min. As in the original study (Gordon et al., 2017), the data of one participant were excluded from the analysis because of excessive motion in the scanner.

The HCP-D resting-set dataset used for replication included participants aged 5–21 years old. The scanning parameters, described in detail by Harms et al. (2018), were very similar to the protocol used in HCP-YA. Resting-state run duration was 6.5 min (488 volumes). In our analysis, we used only those participants undergoing two runs per

day on two different days. After preprocessing (see below) and segmenting the data into windows (see below), our data for "Gap 0 s" analysis included 472 participants (age mean, 15.35 years; age SD, 3.68 years; 260 females) and for "Gap different days" analysis included 432 participants (age mean, 15.43 years; age SD, 3.69 years; 237 females). Using the HCP-D dataset, we examined only the periods of "Gap 0 s" and "Gap different days" because the run's duration in the HCP-D dataset was much shorter than that in the HCP-YA dataset. The HCP-D dataset also includes a variety of behavioral measures acquired outside the scanner.

Data analysis. The data were analyzed using MATLAB and homemade scripts (Axelrod, 2014). A detailed description of the HCP-YA preprocessing pipeline has been provided earlier (Glasser et al., 2013). We used the outputs of the minimal preprocessing pipeline that included data denoising using independent component analysis (ICA) and FMRIB's ICA-based X-noiseifier (Griffanti et al., 2014). HCP minimal preprocessing pipeline might not sufficiently eliminate motion-related artifacts (Burgess et al., 2016; Siegel et al., 2017), so as an additional step, we applied a "scrubbing" procedure. Specifically, following the recommendation of Power et al. (2012), we censored the frames with frame displacement (FD) values >0.2 mm. We excluded 20 participants for whom >70% of frames were censored. Note that we also conducted a series of control analyses to ensure that motion artifacts cannot potentially explain the neural persistence results (see further in the text). The processing procedures of the HCP-D were the same as those of the HCP-YA. The HCP pipeline uses surface-based brain image registration, which is a robust registration method for the pediatric population across ages (Ghosh et al., 2010; Levman et al., 2017; Hagler et al., 2019).

The fully preprocessed MSC dataset has been downloaded from https://openneuro.org/datasets/ds000224/versions/1.0.3. Full details regarding processing steps can be found in the original publication (Gordon et al., 2017). Briefly, the data were confound-regressed and motion-censored (i.e., frames with FD values >0.2 mm were censored). The procedures for surface processing and CIFTI generation of the MCS dataset were similar to the HCP-YA and HCP-D datasets (Glasser et al., 2013). The MSC dataset was used for a single analysis only to examine persistence over a longer run time duration.

Network connectivity analyses. We used a multimodal parcellation atlas (HCP-MMP; Glasser et al., 2016) to parcellate the cerebral cortex into a set of ROIs. The HCP-MMP includes 180 ROIs per hemisphere. For each ROI, the resting-state time-course was extracted. Time-varying functional connectivity was estimated between pairs of time-courses using a sliding-window approach. For our main analysis, we used a window length of 2.88 min with 0.288 min of overlap. This window length was relatively long and much longer than is usually used in so-called "dynamic" time-varying functional connectivity analyses (Allen et al., 2014; Zalesky et al., 2014; Leonardi and Van De Ville, 2015; Laumann et al., 2017). In addition, we replicated our results using control analyses with a window length of 1 min (no overlap) and 5 min (0.49 min overlap). The latter analysis used a window length comparable to the run duration used in so-called static connectivity analyses (Noble et al., 2019). Thus, the controversies related to dynamic functional connectivity (e.g., sampling variability) cannot explain our results (Hutchison et al., 2013; Laumann et al., 2017; Lurie et al., 2019).

For each time window, the network was estimated by calculating pairwise Pearson's correlations between the time-courses of all pairs of ROIs (nodes). As a thresholding procedure, to establish whether the link between two nodes was sufficiently strong, we used an established method (Berezin et al., 2012; Ludescher et al., 2013; Wang et al., 2013) to estimate how much a correlation between pairs of nodes "stands out" from background noise. Specifically, the procedure was as follows. First, we calculated the cross-correlation between time-courses of two nodes; correlation at $t = 0$ (i.e., no displacement between time-courses) is denoted as $R_{t=0}$. Second, we calculated the average [denoted as $\mathrm{Avg}(R_{t\neq 0})$] and standard deviation [denoted as $\mathrm{Std}(R_{t\neq 0})$] of correlation values at all time points, excluding $t = 0$. As the final step, for each pair of nodes we calculate the link significance W as follows:

$$W = \frac{R_{t=0} - \mathrm{Avg}(R_{t\neq 0})}{\mathrm{Std}(R_{t\neq 0})}.$$

The meaning of W is, thus, how many SD the cross-correlation value of the link stands out above the level of noise. We retain the link if W is above a $W_{\mathrm{Threshold}}$. A single (i.e., universal) $W_{\mathrm{Threshold}}$ was used for all participants, time windows, and links. To avoid any potential circularity of the analysis (Kriegeskorte et al., 2009), $W_{\mathrm{Threshold}}$ was established using the data of 20 independent participants (i.e., these data were not part of the main analysis dataset). We established the $W_{\mathrm{Threshold}}$ using the following procedure. First, for each of the 20 participants, time window, and pair of nodes, we calculated W as described above. Second, for each participant, we randomized the time-courses of each node within every time window. Subsequently, for each pair of nodes, we computed W_{Shuffle} using the same methodology employed to obtain W. For both W and W_{Shuffle}, we plot probability density distributions in a log–log scale (Fig. 1). We choose the $W_{\mathrm{Threshold}}$ equal to 3.5, the value for which the probability density of W is 100 times larger than W_{Shuffle} (i.e., a false-positive rate of 1%). Note that we obtained qualitatively similar results when $W_{\mathrm{Threshold}} = 3$, $W_{\mathrm{Threshold}} = 4$, and $W_{\mathrm{Threshold}} = 4.5$ were used.

Note that the $W_{\mathrm{Threshold}}$ was a single threshold for all participants. Accordingly, the number of retained links per participant varied. To rule out the possibility that this biased our results, we repeated the analysis while retaining the same (i.e., fixed) number of links per participant (7.5% of links). In addition, we obtained qualitatively similar results in a control analysis using an unthresholded network with all links (more details are provided below).

Network time persistence in our study was evaluated using two methods: links' time persistence and nodes' time persistence analysis. To calculate links' time persistence, the network was first binarized, and then the fraction of identical links in the two networks at two time points of interest was calculated using the Jaccard index. Nodes' time persistence was calculated based on the networks without binarization (i.e., weighted networks) as the similarity of nodes' weighted degree between two time points. Specifically, we calculated the weights first at two time points of interest for each node of the network; then, we calculated a Pearson's correlation between the two vectors of weights between two time points. For the control analysis, we calculated the similarity between two unthresholded networks by calculating the correlation (Pearson's correlation) between connectivity matrices. In our analysis, we examined network persistence over different time intervals. Specifically, the smallest time interval was Gap 0 s (i.e., comparison of all possible two adjacent, nonoverlapping time windows). The maximal time internals (i.e., gaps) within a run that could be estimated reliably were 6.91 min (HCP-YA dataset) and 22.88 min (MSC dataset). Finally, the longest time interval was "Gap different days" (i.e., comparison of time windows between days). For each gap, we calculated and then averaged the similarity of networks for all possible window pairs, resulting in a single value per gap/participant. For reference, we calculated network similarity between time windows of different subjects (i.e., one window in one subject and another window in the other subject) and network similarity for time windows of random networks, which we obtained by shuffling the links in each network. To compare network persistence values of different gaps, we used repeated-measure ANOVA. In case the sphericity assumption was not satisfied, we used a Greenhouse–Geisser correction. Post hoc comparisons were conducted using paired two-tailed and two-sample two–tailed t tests.

We placed special emphasis on ensuring that the network time persistence results might not be explained by the head motion in the scanner. As we described above, we used a state-of-the-art "scrubbing" procedure (0.2 mm threshold). Critically, to further rule out the potential confounding effect of motion, we conducted a series of control analyses. In particular, for both links' and nodes' time persistence analysis, we correlated (and found no correlation) between individual persistence values and (1) mean FD values and (2) absolute head motion distance of the

participant calculated based on the realignment preprocessing outputs. In addition, we repeated our main analyses using data of 100 participants with the lowest head motion artifacts according to FD values. Finally, to further minimize potential confounding motion effects in the scanner, we repeated our analysis using a longer time window of 5 min, the run length used in static connectivity analyses (Noble et al., 2019). In both control analyses, the results were similar to those reported in the main text.

The analysis comparing between network time persistence between different functional networks [e.g., default mode network (DMN), visual network] within the same brain was conducted using the HCP-YA dataset and replicated using the HCP-D dataset. For this analysis, we assigned the nodes to networks based on well-established functional network parcellation (Yeo et al., 2011). The estimation of links and node network time persistence is inherently influenced by the number of nodes and links of the network. Accordingly, given that the brain's functional networks are of different sizes (i.e., they contain different numbers of nodes and links), the comparison between the functional networks "as is" would have been biased. To address this, after thresholding we randomly selected a fixed and the same number of links in each network. The analysis was repeated 300 times with the number of nodes fixed at 34 (which corresponds to the smallest network) selecting different nodes each time. At the end of the procedure, we averaged the results. The number of links used in the main text analysis was 25, while very similar results were obtained using 50 and 100 links. We also conducted replication analysis using the HCP-D dataset using 25 links. We omitted the limbic network from our analysis because the percentage of retained links in this network was disproportionately (i.e., about five times) lower than in other networks. Given that the limbic network is a priori a small network, the number of nodes and links after thresholding in the limbic network was too low for reliable analysis.

To test whether the network time persistence is heritable, we used a standard twin design (Ebstein et al., 2010) to examine the similarity of 115 monozygotic and 60 dizygotic twin pairs. Zygosity information was genotype-verified by the HCP consortium. For each twin group, we correlated the values of network time persistence across twin pairs. We used Pearson's correlation (similar results were obtained using Spearman correlation). Similar to our previous studies (Mizrahi and Axelrod, 2023; Baranes et al., 2024), the significance correlation within each twin group was established using the bootstrap resampling method (Wilcox, 2012). The comparison of correlations was also conducted using a bootstrap method (https://github.com/GRousselet/blog/tree/master/compcorr). We used 10,000 bootstrap sets in all bootstrap analyses. To validate that the similarity of motion in the scanner between twins does not explain our results, we conducted a partial correlation analysis in which we used a vector of scanner motion similarity of twin pairs as a confounding variable. Specifically, for each twin pair, we calculated the absolute difference in the number of excluded frames based on the FD parameter.

To examine the association between network time persistence and behavior, we used 239 behavioral HCP-YA measures spanning a variety of domains such as cognition, sensory emotional processing, and personality. Note that our goal was not to make claims about the correlation of a specific variable, but rather to examine in general whether network time persistence and behavior are associated. For that, our critical analysis was to examine whether the total number of high correlations ($p < 0.05$, uncorrected) is beyond the number of high correlations that can be expected by chance. Specifically, to obtain surrogate distribution, (1) for each neural persistence/behavioral score pair, we reshuffled the data to disrupt the relationship and computed the correlation; (2) we calculated the total number of significant correlations; and (3) we repeated steps (1) and (2) 1,000 times to obtain the distribution of the number of significant correlations for the shuffled data. Recently, the concerns regarding the reliability of brain–behavior correlations (Marek et al., 2022) have been raised [but see also DeYoung et al. (2022); Makowski et al. (2023); Spisak et al. (2023)]. Our overall goal was not to make claims about the correlation of a specific variable, and thus the concerns raised by Marek et al. (2022) are less or not at all applicable to our results. Critically, we also replicated our findings using the HCP-D dataset by examining the correlation between network time persistence and 145 behavioral measures (different measures than in the HCP-YA dataset), spanning a variety of domains such as sensory processing, executive function, language, emotions, working and episodic memory, personality, and psychopathology.

Results

In our analysis, we primarily used the HCP-YA resting-state dataset (954 subjects; run duration, 14.4 min). We extracted time-courses from 360 cortical ROIs based on Glasser and colleagues' parcellation (Glasser et al., 2016). We segmented the data into windows of 2.88 min (0.288 min overlap) and constructed the network for each segment as a pairwise correlation between the ROIs. We conducted the network analysis for the strongest links by retaining links with connectivity substantially beyond the background noise (for full details, see Materials and Methods and Fig. 1). The average percentage of retained links per participant was 7.5% (SD, 4.0%). We quantified the time persistence of the network using two measures: links' time persistence (i.e., the fraction of links that remain the same for both time points; Fig. 2*A*) and nodes' time persistence (i.e., the similarity of nodes' weighted degree between two time points; Extended Data Fig. 2-1*A*). We also replicated our results using an unthresholded network (see below). For full methodological details, see Materials and Methods.

Network time persistence for time gaps of an increasing length

To explore network time persistence, we first compared the network structures for three intervals of time (i.e., gaps): all possible pairs of adjacent and nonoverlapping windows within the same run ("Gap 0 s"), all possible pairs of windows with the time gap of 7.78 min ("Gap 7.78 min"), and all possible windows across 2 proximate days ("Gap different days"). The results of the links' persistence analysis are shown in Figure 2*B* (gray bars), and we can see that the network resembles itself less as the gap increases. Statistically, repeated-measure ANOVA with "gap" as a factor revealed a major main effect of the gap ($F_{(1.834,\ 1,748)} = 1{,}689$; $p < 0.001$; $\eta^2 = 0.64$). A post hoc paired t test revealed a major difference between all three conditions ($p < 0.001$; Cohen's $d > 0.63$). For reference, we also examined network similarity between time windows of different subjects (i.e., one window of a pair in one subject and another window of a pair in the other subject) and network similarity for time windows of random networks (Fig. 2*B*, white bars). We can see that the functional network of the same subject even across different days (i.e., "Gap different days") resembled itself much more than the networks of two different participants ($t_{(1,906)} = 28.1$; $p < 0.001$; Cohen's $d = 1.29$). Yet, the functional networks of the different participants were more similar to each other than random networks ($t_{(1,906)} = 53.3$; $p < 0.001$; Cohen's $d = 2.44$). To zoom in and to explore network change over a shorter timescale, we examined network changes within a single run across eight equidistant time points. We can see (Fig. 2*C*) that over a short timescale within the same run, the network also becomes gradually less similar to itself as time passed. Using repeated-measure ANOVA, we found a statistically significant main effect of the gap ($F_{(1.5,\ 1,434)} = 297.9$; $p < 0.001$; $\eta^2 = 0.238$), while there was also a strong linear trend ($F_{(1,953)} = 364.9$; $p < 0.001$; $\eta^2 = 0.277$). So far, we have used HCP data with a run duration of 14.4 min. To test the network change over a longer run, we used the MSC dataset (Gordon et al., 2017), in which the participants underwent resting-state scanning with a run duration of 30 min (see Materials and Methods for full details). Using links' persistence analysis, we

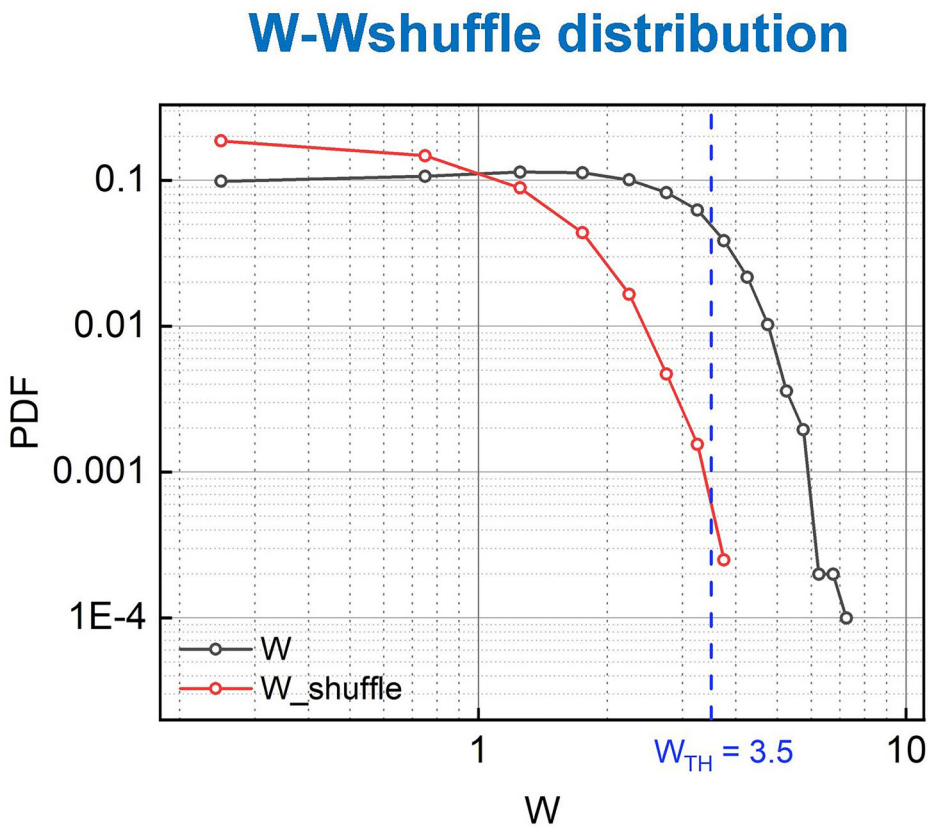

Figure 1. Illustration of $W_{Threshold}$ selection. Probability density distributions for W and $W_{Shuffle}$ were calculated based on the data of 20 subjects; these data were not part of the main analysis dataset. W (in black) and $W_{Shuffle}$ (in red) are plotted in the log–log scale. We choose the $W_{Threshold}$ equal to 3.5, the value for which the probability density of W is 100 times larger than $W_{Shuffle}$ (i.e., false-positive rate of 1%).

found a gradual decrease in network similarity up to the maximal tested duration of 22.88 min (Fig. 2*D*). Statistically, repeated-measure ANOVA revealed a significant main effect of the gap ($F_{(1.84,\ 14.7)} = 10.27$; $p = 0.002$; $\eta^2 = 0.562$) with a strong linear trend ($F_{(1,8)} = 14.7$; $p = 0.005$; $\eta^2 = 0.648$). Notably, network similarity continued to decrease when "Gap different days" was considered (paired t test between "Gap 22.88 min" and "Gap different days", $t_{(8)} = 3.69$; $p = 0.006$; Cohen's $d = 1.23$). To complement the links' time persistence analysis, we conducted a nodes' time persistence analysis, which focuses on the degree of nodes (see Materials and Methods). Links' and nodes' time persistence measures are sensitive to different aspects of network properties and therefore might not necessarily agree. For example, the exchange of links within the network diminishes links' persistence but might not change nodes' persistence. The results of the nodes' persistence analysis (Extended Data Fig. 2-1) were qualitatively similar to the links' persistence analysis (Fig. 2), suggesting potentially similar mechanisms. To examine the similarity between two types of measures more directly, we calculated the across-subject correlation between links' and nodes' persistence values, and the correlation was indeed high (Extended Data Fig. 2-2). Finally, it was important to ensure that our results were not idiosyncratic to specific network definitions and parameters used. To address this, we conducted a series of control analyses. First, given that a single threshold ($W_{Threshold}$) was used for all participants, the number of retained links per participant varied. To rule out that this might bias the results, we repeated the analysis, retaining the same (i.e., fixed) number of links (7.5%) for each participant (Extended Data Fig. 2-3). Second, we repeated the analysis using shorter time window of 1 min (Extended Data Fig. 2-4*A*) and longer time window of 5 min (Extended Data Fig. 2-4*B*). Third, we repeated the analyses using different thresholds for network thresholding (Extended Data Fig. 2-5). Fourth, we repeated the links' time persistence analysis using an unthresholded network (Extended Data Fig. 2-6). Critically, the results across all analyses were qualitatively similar to the main result analysis (Fig. 2).

We have shown so far that the network resembles itself less as time passes, but the potential concern is whether our effect cannot be explained by the head motion artifacts of the participants in the MRI scanner. Critically, as we show below, motion artifacts were unlikely to have had a major impact on our results. First, in our analyses we employed a state-of-the-art "scrubbing" procedure (i.e., exclusion of frames with an FD value >0.2 mm; Power et al., 2012), which minimizes any potential head motion influence on the results at the neural level. Second, we found no correlation in a set of control analyses (Extended Data Fig. 2-7) between individual time persistence values and (1) mean FD values and (2) absolute head motion distance of the participant. Third, we replicated our main analysis results when we included only 100 participants with the lowest head motion according to FD values (Extended Data Fig. 2-8). Finally, as we have already reported above, we reproduced our results in the analysis with a window length of 5 min (Extended Data Fig. 2-4*B*), suggesting that the motion confounds, which might have more serious consequences in "dynamic" connectivity analyses (Laumann et al., 2017; Lurie et al., 2019) cannot explain our results. Overall, it is thus highly unlikely that the motion artifacts explain our results.

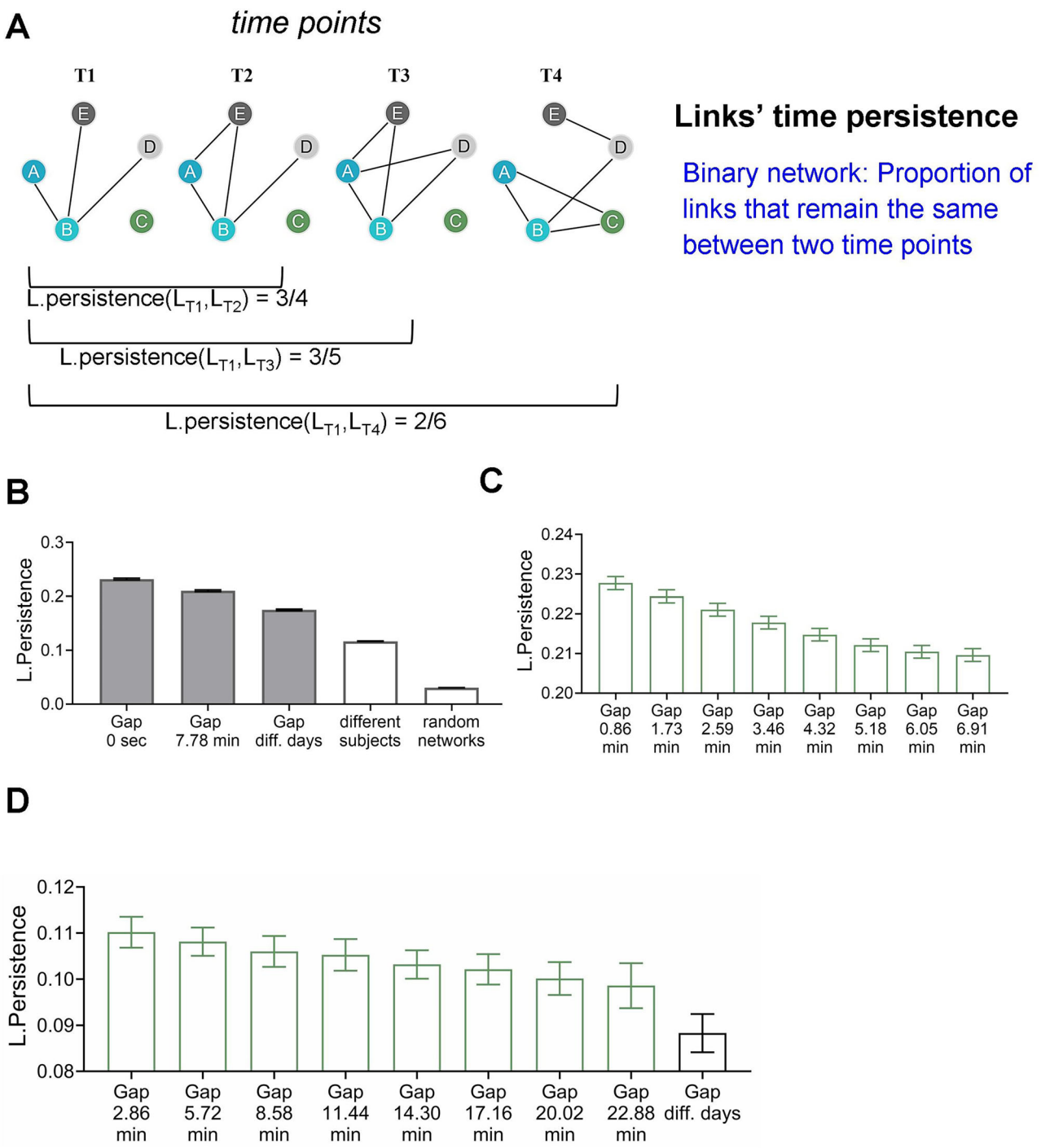

Figure 2. Network time persistence at links level across gaps within the run and across days. ***A***, Demonstration of calculating the links' persistence. Links' persistence is calculated using the Jaccard coefficient as a fraction of links that remains the same between two time points. Notably, some links exhibit stability, while others disappear, resulting in a decrease in the network's similarity with an increasing gap (in our toy example, from 3/4 to 3/5 and then to 2/6). ***B***, Group-level network time links' persistence within a run and between days (HCP-YA dataset). The five conditions are "Gap 0 s" (i.e., consecutive time windows within the same subject), "Gap 7.78 min" (i.e., the gap of 7.78 min within the same run and subject), "Gap different days" (i.e., windows across different days of the same subject), different subjects, and random brain networks constructed from the shuffled fMRI data of different subjects. Note that the network gradually becomes less similar to itself with the larger gap, progressing from most similar at "Gap 0 s" to less similar "Gap different days" gap (gray bars). "Gap different days" exhibited much higher network similarity to itself than "different subjects" and even more so compared with "random networks." ***C***, Group-level network time links' persistence within the run (HCP-YA dataset). The maximal gap that could be examined was 6.91 min. Note that network similarity gradually decreased with time. ***D***, Group-level network time links' persistence within a relatively long run and across different days (MSC dataset). Note that network similarity gradually decreases as the gap time length increases. In all subplots here and consecutive figures, error bars represent the standard error of the mean. Results of the nodes' persistence analysis and across-subject correlation between links' and nodes' persistence values are shown in Extended Data Figures 2-2 and 2-3, respectively. Links' and nodes' persistence control analyses for different network definitions and parameters are presented in Extended Data Figures 2-4–2-14.

The within-run analysis was conducted using all possible pairs of adjacent and nonoverlapping windows, but a potential concern is that the decreased network similarity that we found was driven specifically by the period at the beginning of the run. That is, if, for example, due to psychological and/or physiological novelty of the situation, brain network dynamics at the

beginning of the scan is more variable, this might cause a decrease in network similarity specifically at the beginning of the run. To test this possibility, we conducted a series of control analyses in which we repeated the analysis by excluding the data at the beginning of a run (i.e., three separate analyses: excluding the first minute, excluding the first 3 min, and excluding the first 5 min of a run; similar results were obtained when the first 2 and 4 min of a run were excluded). The results of this analysis are shown in Extended Data Figure 2-9 (links' analysis) and Extended Data Figure 2-10 (nodes' analysis), and we can see that network similarity gradually decreased as the time gap length increased, mimicking the results of our main analysis with a full run (Fig. 2; Extended Data Fig. 2-1). To obtain further empirical support that the decrease in network similarity was not driven specifically by the data at the beginning of the run, we calculated across-participant correlation between the results obtained using full run and when the data were excluded at the beginning of a run. For both links' persistence (Extended Data Fig. 2-11) and nodes' persistence analyses (Extended Data Fig. 2-12), we found high correlation, supporting the notion that the decrease in network similarity was not driven specifically by the data at the beginning of the run. We also observed that the correlation with full run decreased when the larger period at the beginning of the run was excluded, but this phenomenon was unrelated to variable network dynamics at the beginning of a run and was likely related to the fact that excluding a larger period decreased the amount of data in the analysis, resulting in more variable results. Indeed, repeating the analysis by excluding the periods at the end of the run (instead of those at the beginning) yielded similar decrease in correlation as the larger period was excluded (Extended Data Figs. 2-13, 2-14). Overall, our analyses showed that the decreased network similarity could not be explained by more variable brain network dynamics at the beginning of the run.

Differences in network time persistence between functional networks of the same brain

So far, we analyzed the network time persistence of the whole brain, but the brain comprises different functional networks (Power et al., 2011; Yeo et al., 2011). Accordingly, we asked whether and how network time persistence varies across functional networks within the brain. Based on the functional network parcellation of Yeo et al. (2011), we calculated network time persistence for different functional networks. The results for links' and nodes' network time persistence are shown in Figure 3*A*, and we can see that functional networks differed with regard to network time persistence. The effect was confirmed statistically by finding a highly significant main effect of a network in the repeated-measure ANOVA (links persistence analysis, $F_{(4.11,\ 3,895)} = 1{,}429$; $p < 0.001$; $\eta^2 = 0.6$; nodes persistence analysis, $F_{(4.45,\ 4{,}244.1)} = 1{,}129$; $p < 0.001$; $\eta^2 = 0.54$). Interestingly, the highest network time persistence was observed in the visual and somatomotor networks—the two sensory processing functional networks. The effect was observed in the links' network time persistence analysis (Fig. 3*A*, left) but was even more pronounced in the nodes' network time persistence analysis (Fig. 3*A*, right). For both links' and nodes' persistence analyses, the effects were confirmed statistically: for visual and somatomotor networks, time persistence was higher than for nonsensory networks (links persistence analysis, $t_{(953)} > 28.16$; $p < 0.001$; Cohen's $d > 0.91$; nodes persistence analysis, $t_{(953)} > 38.5$; $p < 0.001$; Cohen's $d > 1.26$). The analyses described above were conducted for "Gap 0 s," but we obtained very similar results for "Gap 7.78 min" and "Gap different days" (Extended Data Fig. 3-1). Note that because the measures of link and nodes' time persistence are sensitive to the number of links, the analyses and the comparison described above could only be conducted for an equal number of nodes per network. Accordingly, the analyses described above were conducted by randomly sampling 25 links for each network (see Materials and Methods for full details). Critically, we fully replicated the results using 50 and 100 links per network (Extended Data Fig. 3-2). To complement the within-network analyses, we also examined network time persistence between functional networks. For the between functional networks analysis, the network is constructed using the links connecting between two networks of interest. The results of between and within functional networks analysis for "Gap 0 s" are shown in Figure 3*B* (see Extended Data Fig. 3-3, for "Gap 7.78 min" and "Gap different days" analyses). We can clearly see that the network time persistence varied substantially between functional networks. Interestingly, the network time persistence within the networks (i.e., average values on the diagonal) was much higher than between the networks [i.e., average values below and beyond the diagonal; specifically, links' persistence, mean within networks, 0.43 (SD, 0.08); mean between networks, 0.26 (SD, 0.09); $t_{(953)} = 99.3$; $p < 0.001$; Cohen's $d = 3.2$; nodes' persistence, mean within networks, 0.57 (SD, 0.09); mean between networks, 0.49 (SD, 0.09); $t_{(953)} = 43.1$; $p < 0.001$; Cohen's $d = 1.39$].

To replicate our findings in an independent way, the same set of analyses was repeated using the large open-access HCP-D dataset analyzed the same way (see Materials and Methods). Remarkably, using HCP-D dataset, we obtained very similar results (Extended Data Fig. 3-4). Statistically, correlation of the within and between networks between HCP-YA and HCP-D was very high: "Gap 0 s," links' persistence, $R = 0.98$; $p < 0.001$; confidence interval (CI), [0.961–0.996]; "Gap 0 s," nodes' persistence, $R = 0.9$; $p < 0.001$; CI, [0.734–0.971]; "Gap different days," links' persistence, $R = 0.99$; $p < 0.001$; CI, [0.986–0.997]; and "Gap different days," nodes' persistence, $R = 0.96$; $p < 0.001$; CI, [0.924–0.985].

Individual differences in network time persistence

Our analyses thus far investigated network time persistence at the group level. Next, we examined individual variability of network time persistence. In Figure 4*A*, for illustrative purposes, we show the time persistence values of eight representative individuals for different within-run time intervals and different days. We can see that participants who showed low network time persistence for a smaller gap tended to also have low network time persistence for the larger gap and vice versa, suggesting that participants likely have their characteristic network time persistence. To test the effects quantitatively using our full dataset (i.e., 954 participants), we correlated individual time persistence values across different time intervals. We found (Fig. 4*B*) a very high correlation between the network time persistence for different intervals within the same run, "Gap 0 s" versus "Gap 4.03 min" ($R = 0.92$; $p < 0.001$; CI, 0.90–0.93) and "Gap 0 s" versus "Gap 7.78 min" ($R = 0.75$; $p < 0.001$; CI, 0.72–0.77), as well as for the interval within run and between days, "Gap 7.78" versus "Gap different days" ($R = 0.79$; $p < 0.001$; CI, 0.75–0.81). We also found high correlations for additional intervals within the same run, using both links' and nodes' persistence analyses (Extended Data Fig. 4-1). In addition, we found that the individual time persistence for the same time interval measured on two different days was similar (Fig. 4*C*): "Gap 0 s" ($R = 0.60$; $p < 0.001$; CI, 0.56–0.65)

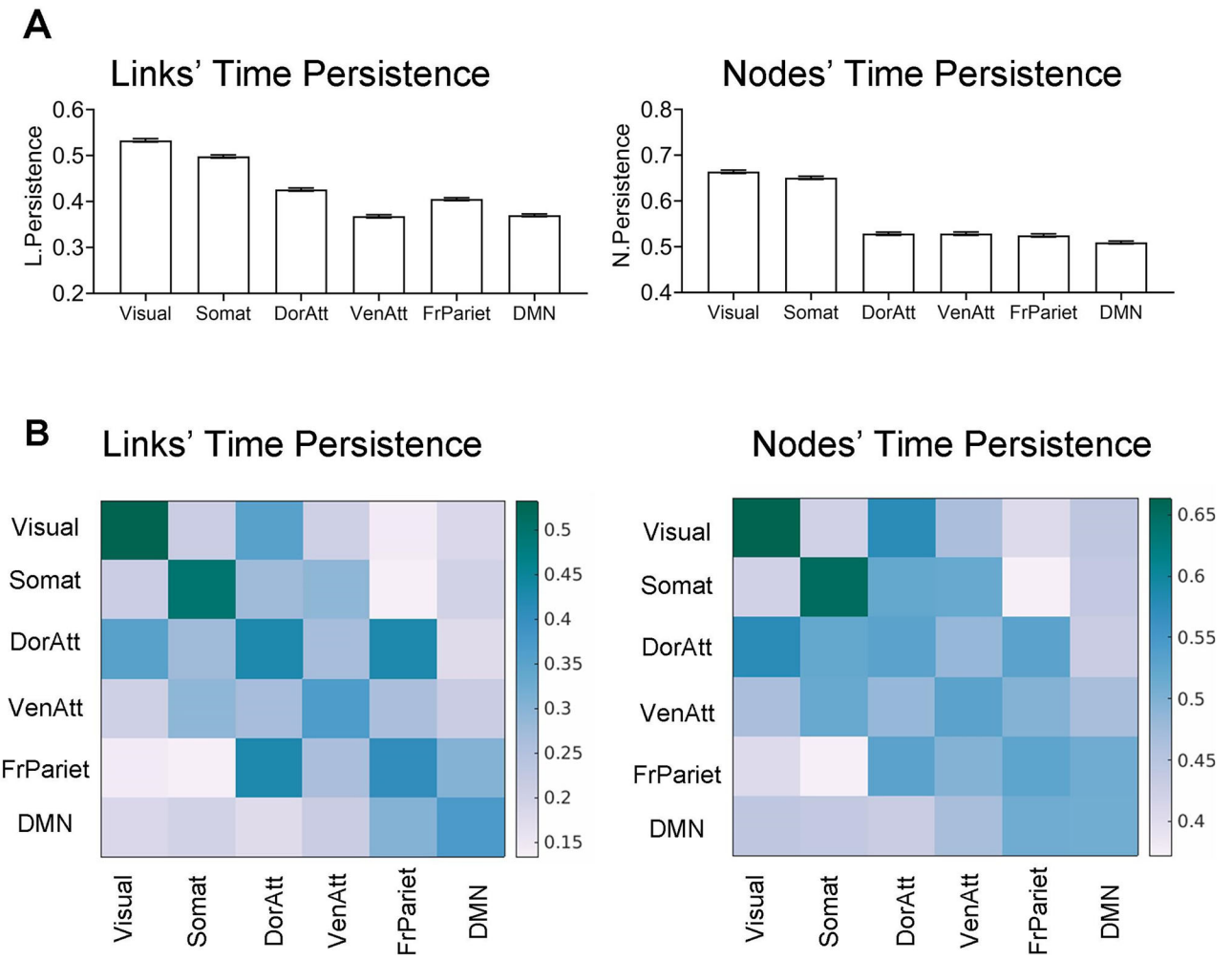

Figure 3. Network time persistence across functional networks ("Gap 0 s"). ***A***, Comparison of within-network persistence for links' time persistence (left) and nodes' time persistence (right). "Somat" stands for the somatomotor network, "DorAtt" stands for the dorsal attention network, "VenAtt" stands for the ventral attention network, "FrPariet" stands for the frontal parietal network, and "DMN" stands for the default mode network. Note higher persistence values in the two sensory networks (i.e., visual and somatomotor networks). Interestingly, the dissociation between two sensory networks and nonsensory networks was stronger in nodes' than in links' time persistence. Results for "Gap 7.78 min" and "Gap different days are shown in Extended Data Figure 3-1. The results using 50 and 100 links per network are shown in Extended Data Figure 3-2. ***B***, Within networks (diagonal) and between networks (off-diagonal), network time persistence for links' time persistence (left) and nodes' time persistence (right). Darker colors reflect higher persistence values. Note that network time persistence varied substantially within and between networks. Also note that the network persistence within networks (diagonal values) was much higher than between networks (beyond or below diagonal values). Results for "Gap 7.78 min" and "Gap different days" are shown in Extended Data Figure 3-3. Results of replication analysis using HCP-D dataset are shown in Extended Data Figure 3-4.

and "Gap 7.78 s" ($R = 0.49$; $p < 0.001$; CI, 0.44–0.54). High persistence similarity measured on two different days was also found for additional intervals within the same run using both links' and nodes' persistence analysis (Extended Data Fig. 4-2). Overall, this suggests that network time persistence can be considered an individual personal trait.

Genetic origin of individual network time persistence

Given that network time persistence might be an individual trait, is it at least to some extent heritable? Using a standard twin design (Ebstein et al., 2010), we examined whether monozygotic twins (115 pairs) are more similar (i.e., exhibit higher correlation) than dizygotic twins (60 pairs) with regard to network time persistence values. Monozygotic twins share 100% of the genetic material, and dizygotic twins share only 50% of the genetic material; therefore, a higher correlation across monozygotic twins will indicate that the network time persistence is heritable to some extent. As we can see in Figure 5*A* (links' network time persistence analysis) monozygotic twins were highly similar with regard to time persistence for all three time intervals ("Gap 0 s," $R = 0.61$; $p < 0.001$; CI, 0.50–0.7; "Gap 7.8 min," $R = 0.54$; $p < 0.001$; CI, 0.39–0.65; "Gap different days," $R = 0.56$; $p < 0.001$; CI, 0.42–0.68). In contrast, correlation across dizygotic twins (Fig. 5*B*) was low and insignificant ("Gap 0 s," $R = 0.12$; $p = 0.39$; CI, −0.14 to 0.37; "Gap 7.8 min," $R = 0.08$; $p = 0.58$; CI, −0.22 to 0.37; "Gap different days," $R = 0.1$; $p = 0.58$; CI, −0.21 to 0.4). Critically, direct comparison between monozygotic and dizygotic twins using bootstrap permutation analysis revealed a higher correlation in monozygotic compared with dizygotic twins for all three time intervals ("Gap 0 s," $p < 0.001$; CI, 0.21–0.77; "Gap 7.8 min," $p = 0.005$; CI, 0.15–0.77; "Gap different days," $p = 0.003$; CI, 0.14–0.78). We obtained similar results in nodes' time persistence analysis (Extended Data Fig. 5-1). Interestingly, it was previously shown that genetically similar people might have similar head motion artifacts in the scanner (Hodgson et al., 2017). Thus, it was important to rule out the possibility that the similar extent of motion in the scanner of the twins explains their similarity at the level of network time

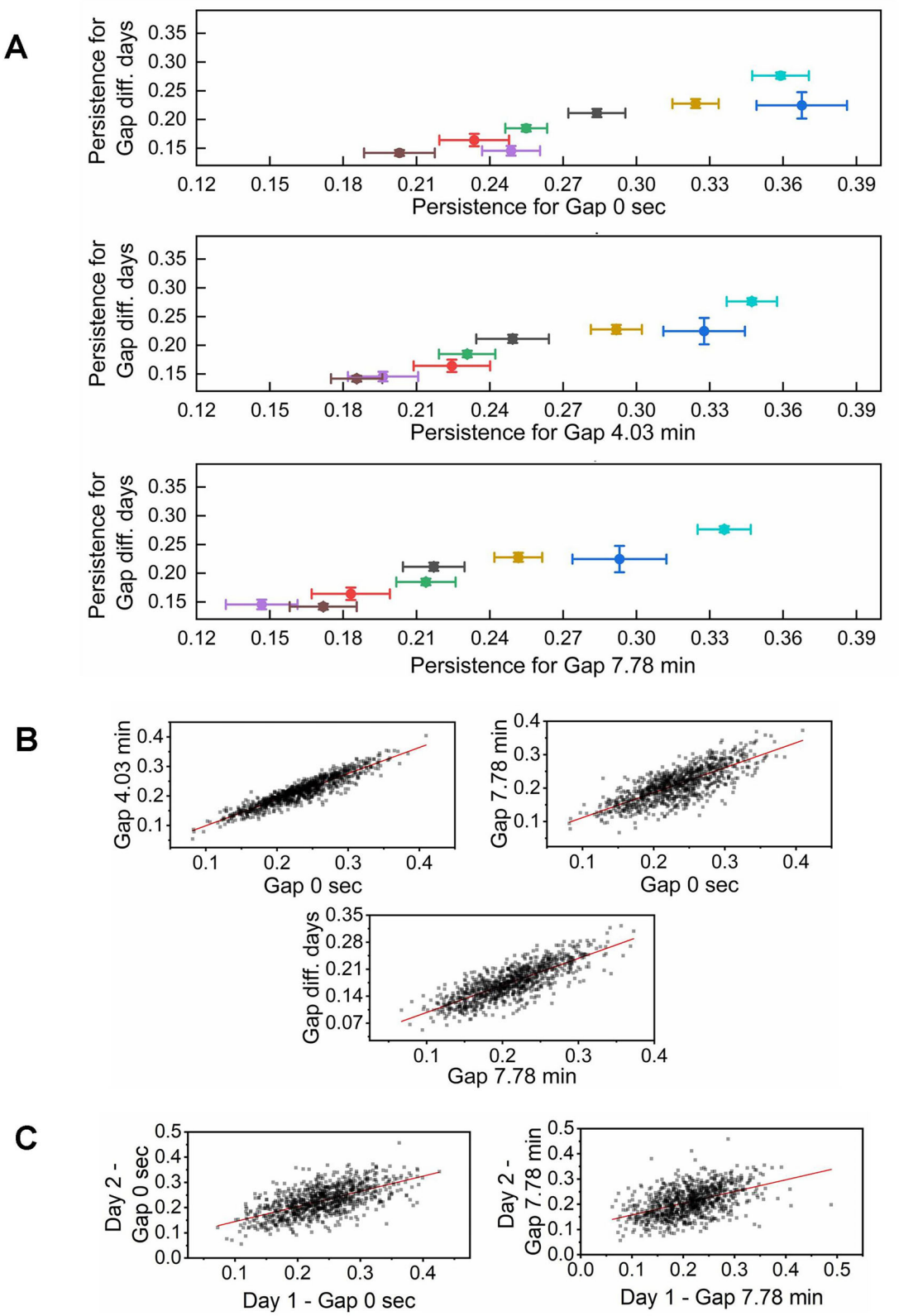

Figure 4. Individual differences in network time persistence (links' persistence). ***A***, An illustrative example of network links' persistence values for eight representative participants. The *x*-axis represents persistence values for various within-run gaps ("Gap 0 *s*", "Gap 4.03 min", and "Gap 7.78 min"). The *y*-axis represents the persistence values of "Gap different days." Each data point reflects individual persistence values and their error bars. The red line is the least-squares line. Note that each participant exhibits characteristic persistence, which gradually declines with increasing gaps. ***B***, Correlation between individual network links persistence values of within-run gaps ("Gap 0 *s*" and "Gap 7.88 min") and "Gap different days." Note the very high correlation between values across the gaps, suggesting that participants with lower persistence values over shorter time gaps tend to exhibit lower persistence over longer intervals and vice versa. Correlations for additional intervals within the same run, using both links' and nodes' persistence analyses, are shown in Extended Data Figure 4-1. ***C***, Comparison of individual network links' persistence values ("Gap 0 *s*" and "Gap 7.78 min") between days. Note that the high correlation between persistence values across the days is reflecting that individual's persistence is a stable phenomenon. Correlations of persistence values on two different days for additional intervals using both links' and nodes' persistence analysis are shown in Extended Data Figure 4-2.

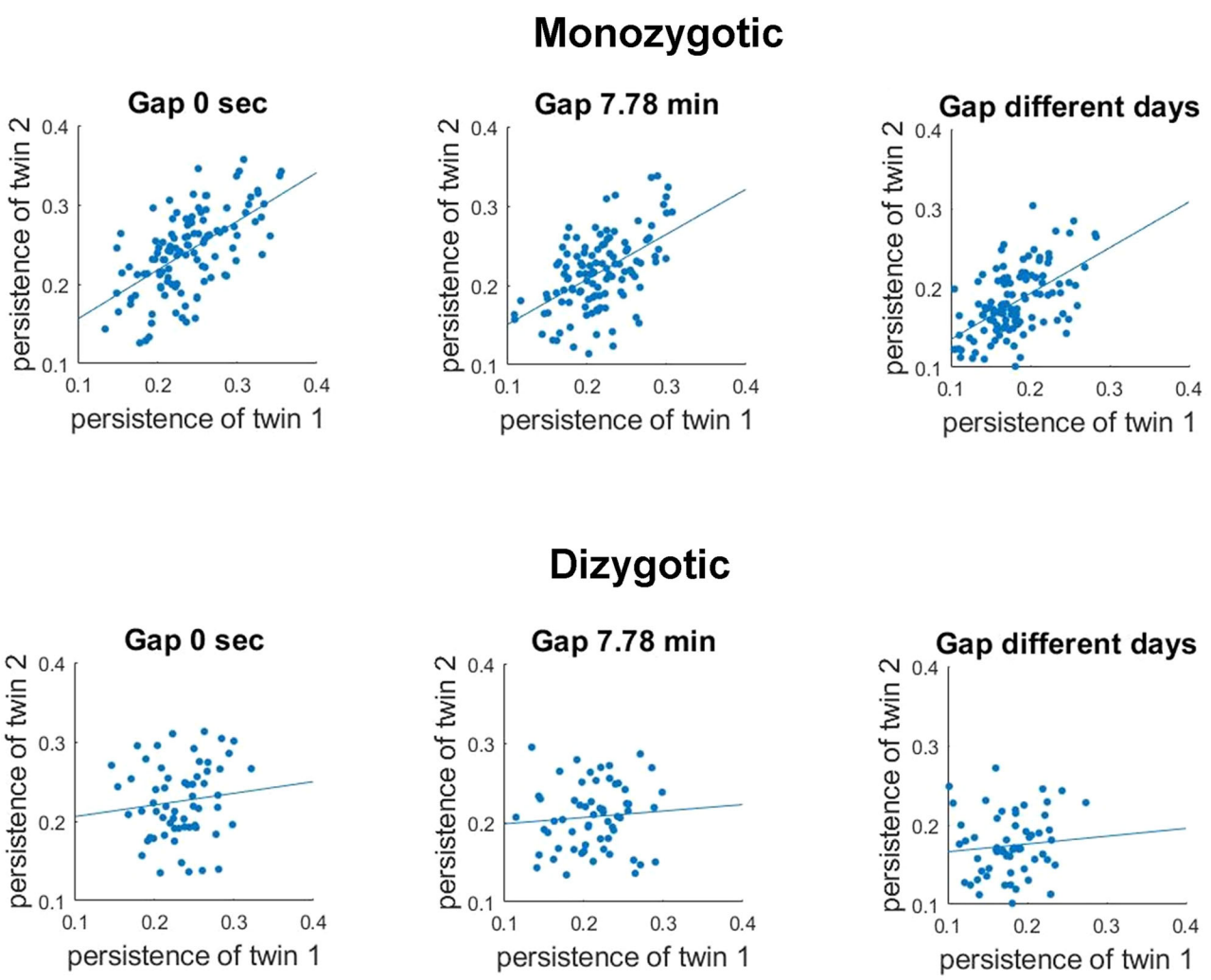

Figure 5. Network time persistence across pairs of monozygotic and dizygotic twins (links persistence). ***A***, Monozygotic twins. ***B***, Dizygotic twins. Columns correspond to three tested gaps: "Gap 0 s," "Gap 7.78 min," and "Gap different days." Each dot reflects the persistence value of the twin pair (i.e., the value on the *x*-axis corresponds to one twin of the pair, and the value on the *y*-axis corresponds to the other twin). The blue line is the least-squares line. High similarity across monozygotic but not across dizygotic twins suggests that network persistence is influenced in part by heredity. Results of nodes' time persistence analysis are shown in Extended Data Figure 5-1.

persistence. For that, we first examined the similarity of FD values between twins and indeed found a correlation of mean FD values for monozygotic twins ($R = 0.39$; $p < 0.001$; CI, [0.18–0.56]). Notably, the correlation was also high for dizygotic twins ($R = 0.35$; $p = 0.009$; CI, [0.07–0.57]), while the correlations between monozygotic and dizygotic groups did not differ ($p = 0.77$; CI, [−0.27 to 0.37]). This latter observation already casts doubt on the idea that motion in the scanner might explain the difference between twin groups in terms of network persistence. To further rule out motion confounding explanations, we repeated our original analysis (Fig. 5*A*) using partial correlation and a vector of scanner motion similarity of twin pairs as a confounding variable. Our results (Table 1) were very similar to those reported in the main analysis, suggesting that motion in the scanner did not have a major impact on our results. We conclude overall that our results indicate that individual network persistence have a genetic component.

Association between individual network time persistence and behavior

We have demonstrated that participants exhibit relatively stable and to some extent heritable individual network time persistence. In our final analysis, we asked whether individual network time persistence can be linked to behavioral performance. To test this, we examined the correlation between network time persistence (whole-brain values) and 239 behavioral measures spanning a variety of cognitive domains such as cognition, sensory, and emotional processing. Note that the main goal of our analysis was not to make claims about the correlation of a specific variable, but rather to examine in general whether individual's network time persistence and behavior are associated. Accordingly, the reliability of specific brain–behavior correlations questioned by Marek et al. (2022) [but see also DeYoung et al. (2022); Makowski et al. (2023); Spisak et al. (2023); Lee et al. (2025)] is less or not at all applicable to our results. The results of our "Gap different days" analysis (links' time persistence) are shown in Figure 6*A*, and we observed significant ($p < 0.05$, FDR multiple-comparison corrected) correlations in several dozen measures (Fig. 6*A*, columns with * sign). For "Gap 0 s" and "Gap 7.78 min," the results were qualitatively similar, if quantitatively weaker compared with "Gap different days" (Extended Data Fig. 6-1). Similar results were also found for all three gaps for the nodes' time persistence measure as was reflected by high correlation between results links' and

Table 1. Partial correlation analysis for monozygotic and dizygotic twins with a vector of scanner motion similarity of twin pairs as a confounding variable

Analysis type	Gap length	Monozygotic twins	Dizygotic twins	Comparison
Links' persistence'	Gap 0 s	$R = 0.59$; $p < 0.001$	$R = 0.14$; $p = 0.32$	$p = 0.002$
		CI, [0.47–0.69]	CI, [−0.14 to 0.4]	CI, [0.16–0.75]
	Gap 7.78 min	$R = 0.53$; $p < 0.001$	$R = 0.09$; $p = 0.56$	$p = 0.009$
		CI, [0.38–0.65]	CI, [−0.19 to 0.38]	CI, [0.11–0.73]
	Gap different days	$R = 0.54$; $p < 0.001$	$R = 0.1$; $p = 0.51$	$p = 0.01$
		CI, [0.39–0.66]	CI, [−0.19 to 0.4]	CI, [0.1–0.75]
Nodes' persistence	Gap 0 s	$R = 0.45$; $p < 0.001$	$R = -0.04$; $p = 0.75$	$p = 0.001$
		CI, [0.32–0.57]	CI, [−0.27 to 0.2]	CI, [0.2–0.75]
	Gap 7.78 min	$R = 0.36$; $p < 0.001$	$R = 0$; $p = 0.99$	$p = 0.04$
		CI, [0.21–0.0	CI, [−0.26 to 0.3]	CI, [0.03–0.66]
	Gap different days	$R = 0.35$; $p < 0.001$	$R = -0.09$; $p = 0.52$	$p = 0.009$
		CI, [0.17–0.52]	CI, [−0.32 to 0.2]	CI, [0.11–0.73]

The third and fourth columns reflect the results of monozygotic and dizygotic twins, respectively. The right-most column reflects the results of the comparison of correlations between the two groups. CI denotes confidence interval. Note: (1) highly significant correlations for monozygotic twins; (2) no correlation for dizygotic twins; (3) significantly higher correlation for monozygotic compared with dizygotic twins.

nodes' network persistence (Extended Data Fig. 6-2). We next proceeded to the key analysis to determine whether the total number of high correlations is beyond what can be expected by chance. Remarkably, using a permutation analysis, we found that for all three gaps the total number of correlations ($p < 0.05$, uncorrected) was significantly higher than those that could be expected by chance (Fig. 6*B*; "Gap 0 s," $p < 0.001$; "Gap 7.78 min," $p = 0.002$; "Gap different days," $p < 0.001$). To replicate these results, we used the HCP-D dataset to examine correlations between network time persistence and 145 behavioral measures from various cognitive domains (see Materials and Methods). Remarkably, as shown in Extended Data Figure 6-3, despite using children rather than adults, our results were similar to those obtained in the main analysis using the HCP-YA dataset. In particular, in the critical analysis, the total number of correlations ($p < 0.05$, uncorrected) was significantly higher than could be expected by chance (Gap 0 s, $p = 0.01$; Gap different days, $p < 0.001$). Taken together, our results show that network time persistence is associated with and possibly even determines behavior.

Discussion

In the present study, we explored the time persistence of the brain's functional network during rest. By devising a new analytical framework and using time gaps both within the run and across days, we established that the functional brain network is persistent, while the network becomes gradually less similar to itself as the time gap increases. Network time persistence also varied across brain functional networks within the same brain, while the sensory networks were most persistent. Exploration of individual differences revealed that participants have individual characteristic persistence that (1) was reproducible across days, (2) was predetermined at least to some extent by genetics, and (3) could be associated with (or linked to) behavioral performance. We elaborate on these findings below.

Time persistence is a fundamental property of many physical and biological systems (Salcedo-Sanz et al., 2022). Here, we conducted a systematic investigation of network time persistence of the human brain. We devised a new approach to estimate network time persistence because the methods used to estimate time persistence at single time-series level, such as DFA (Peng et al., 1994) or Hurst exponent (Hurst, 1951), are not suitable for examining network time persistence. For each time gap, we examined network changes for all possible pairs of windows and then averaged the results. We found that the functional brain network is persistent while network similarity decreased linearly within the run (tested up to 23 min) and continued to decrease across days. Notably, even across days, the network of the same participant was still much more similar to itself than the functional networks of two different subjects (in line with Gratton et al., 2018) or two random networks. Our results were obtained: (1) using links' and nodes' persistence analyses focusing on the strongest links as well as using links' analysis of an unthresholded network; (2) using different thresholds by selecting the strongest links; and (3) using two different datasets. We obtained our results using a short time window (i.e., 1 min) as well as longer time windows (i.e., 2.88 and 5 min), suggesting that potential confounding factors such as sampling variability associated with "dynamic" connectivity analyses (Laumann et al., 2017) cannot explain our results. Our results were also not driven by higher network variability at the beginning of the run. In addition, the analysis parameters that we used and the series of control analyses ensured that our results could not be explained by head motion artifacts in the scanner. All of this inspires confidence that the phenomenon we report here is genuine.

It is important to consider our findings in the context of the dynamic functional connectivity research field (Hutchison et al., 2013; Lurie et al., 2019). It has been well established that the brain exhibits interchangeable connectivity states lasting for several dozen of seconds' duration (Allen et al., 2014; Barttfeld et al., 2015; Vidaurre et al., 2017) and that the transition between states occurs with some probability (Allen et al., 2014; Shappell et al., 2019; Janes et al., 2020; Kringelbach and Deco, 2020). Notably, with regard to understanding network time persistence, analysis of transition between dynamic connectivity states: (1) it is a relatively indirect approach because instead of examining changes in network connectivity per se, it studies changes in states, and (2) it provides only limited information because it examines a relatively short time period of several dozen seconds. Here, using our new approach, we studied network time persistence directly by testing gaps within a run (23 min was the longest within-run gap) and in a between-days gap. Furthermore, compared with studies that examine dynamic connectivity states, our analysis was conducted without any assumptions (e.g., like those of hidden Markov modeling) or constraints (e.g., number of states used in *k*-means clustering). We show that network similarity monotonically decreases with time—a result that could not obviously show up previously by examining transitions between dynamic connectivity states. Our conclusion that the network becomes gradually less similar to itself provides important support for the hypothesis that changes in brain connectivity are ordered and not random (Vidaurre et al., 2017).

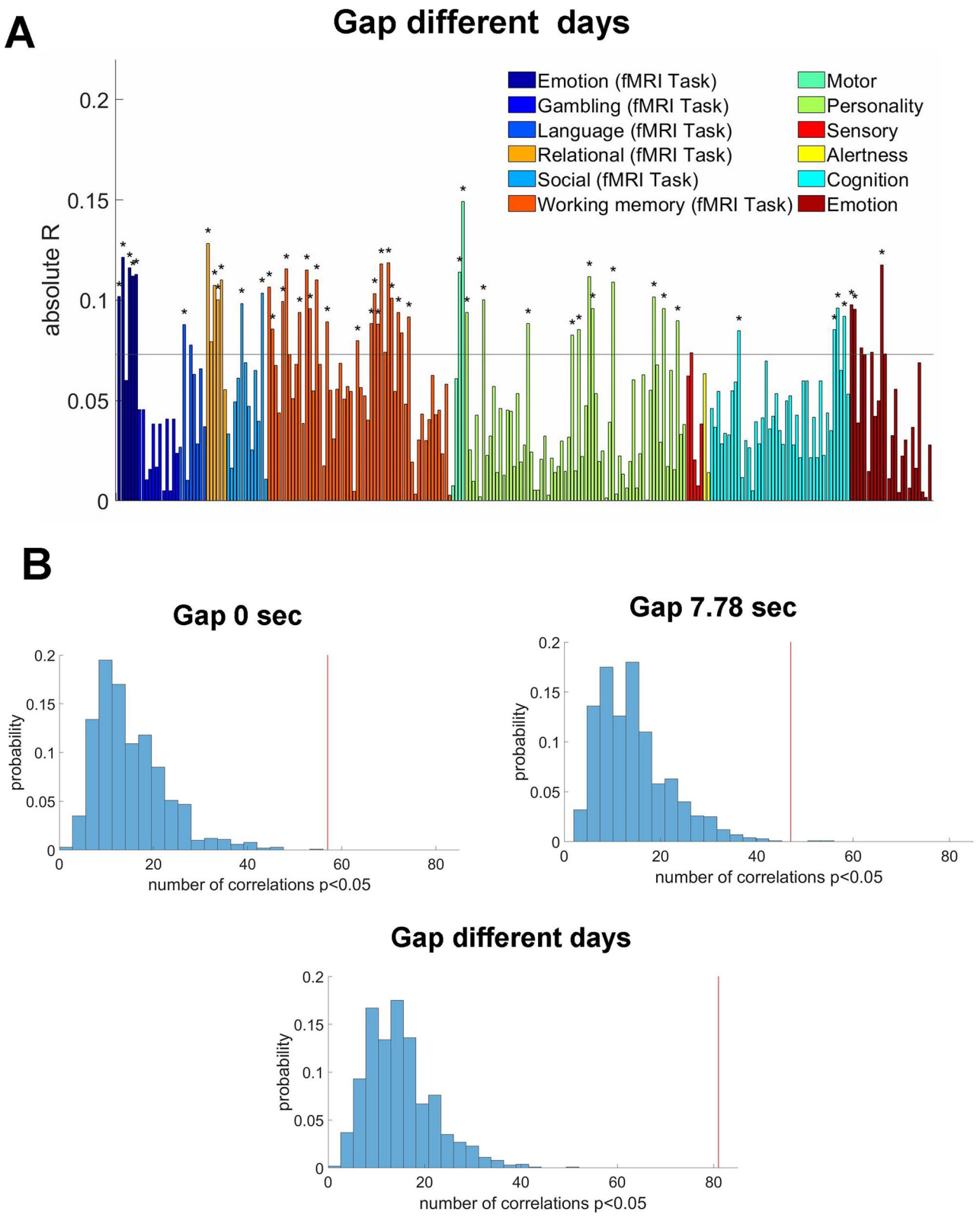

Figure 6. Correlation between network time persistence and behavioral measures. ***A***, Absolute correlation values between link network time persistence ("Gap different days") and 239 behavioral measures. Different cognitive domains are plotted with different colors. Significant correlations ($p < 0.05$; FDR multiple-comparison correction) are indicated with asterisks. The approximate level of $p < 0.05$ uncorrected is indicated with a light gray horizontal line. Note many significant (after the multiple-comparison correction) correlations that spanned different cognitive domains. The results of links' time persistence for "Gap 0 s" and "Gap 7.78 min" are shown in Extended Data Figure 6-1. The results of nodes' time persistence analysis are shown in Extended Data Figure 6-2. ***B***, Permutation correlation analysis of a total number of network persistence versus behavioral measures correlations. We examined whether the total number of high correlations ($p < 0.05$, uncorrected) is higher than can be expected by chance. Note that the number of significant correlations (red vertical line) exceeded what could be expected by chance for all three gaps (i.e., "Gap 0 s," "Gap 7.78 min," and "Gap different days"). The results of replication analysis using HCP-D dataset are shown in Extended Data Figure 6-3.

Beyond examining network time persistence at the level of a whole brain as one functional network, we also found a major difference in network time persistence between different functional networks (Fig. 3). In particular, while the network time persistence of visual and somatomotor networks was the highest, the more high-level processing networks (i.e., dorsal–attentional, ventral–attentional, frontoparietal, and DMN) exhibited lower persistence. This result was found for three gaps we tested (i.e., "Gap 0 s," "Gap 7.88 min," and "Gap different days") and for the different number of links per network (i.e., 25, 50, and 100 links) as well was replicated in two different datasets (HCP-YA and HCP-D). Interestingly, the dissociation between sensory and nonsensory regions was more pronounced in the nodes than in the link analysis, indicating that two measures capture different aspects of network properties. In line with our results, sensory visual (Blautzik et al., 2013; Chen et al., 2015; Shirer et al., 2015; Termenon et al., 2016) and somatomotor (Blautzik et al., 2013; Wisner et al., 2013; Shirer et al., 2015; Termenon et al., 2016) networks have been found to be reliable across "static" resting-state runs. With regard to DMN, the network specialized in internally-directed processing (Axelrod et al., 2017; Buckner and DiNicola, 2019) the reports have been more mixed, while some studies found it reliable (Zuo et al., 2010; Blautzik et al., 2013; Wisner et al., 2013; Termenon et al., 2016), but some did not (Du et al., 2015; Shirer et al., 2015). Critically, while test–retest reliability studies usually use all the links in their analysis, in the present study, we focused on the strongest links, thus potentially increasing the sensitivity of the analysis, permitting it to dissociate between types of networks. The dissociation between sensory and high-level brain networks with regard to network time persistence that we report might reflect a fundamental difference between the networks and their roles in cognition. That is, a higher conscious state has been associated with a larger repertoire of brain states (Barttfeld et al., 2015; Hudetz et al., 2015). Given that high-level regions and networks play a critical role in consciousness and self-related processing (Mashour et al., 2020; Northoff and Lamme, 2020), these areas might have lower network time persistence. Future studies will be needed to provide more support for this hypothesis.

Our network time persistence analysis was conducted for each individual using two measures: links' time persistence (i.e., the fraction of links that remain the same between two time points) and nodes' time persistence (i.e., the similarity of nodes' weighted degree between two time points). It was important to use two different measures because, given that they capture different aspects of network properties, these measures might not necessarily agree. That is, the exchange of links within the network diminishes links' persistence but might not change nodes' persistence (i.e., the node's weight value will not change if one link is replaced with another). Using whole-brain network analysis (Fig. 2; Extended Data Fig. 2-1), we found that the link and nodes' persistence measures were correlated (Extended Data Fig. 2-2), potentially reflecting similar mechanisms. Interestingly, at the level of brain networks, we found an example of a divergence between the two measures, with the dissociation between sensory and nonsensory regions being more pronounced in the node than in the link analysis (Fig. 3*A*). This latter result demonstrates a case where the results of links' and nodes' time persistence analyses reflect potentially different underlying mechanisms. In the future, it would be interesting to investigate more deeply the relationship between the two measures, potentially shedding light on mechanisms underlying brain network dynamics.

An additional interesting aspect of our work was the examination of individual differences in network time persistence. Specifically, we found that individuals have a characteristic network time persistence that was consistent across gaps. For example, individuals with high network time persistence for a gap of 0 s tended to have high network time persistence for a gap of different days. The network time persistence individual values were highly stable, as reflected by our ability to replicate the results in 2 different days. Using a standard twin design, we also found that individual time persistence values were partly genetically predetermined, as monozygotic twins had much more similar network time persistence values than dizygotic twins. Finally, we showed that individual values of network time persistence could be linked to individual cognitive performance, a result replicated across two different datasets. Thus, it is possible that individual's network time persistence contributes at least to some extent to individual cognitive performance. Individual differences in functional connectivity have been explored previously—both the link between functional connectivity and network states to genetics (Glahn et al., 2010; Vidaurre et al., 2017; Jun et al., 2022) and by achieving individual identification as well as decoding individual behavioral and demographic variables (Finn et al., 2015; Smith et al., 2015; Liu et al., 2018). Critically, note that functional connectivity patterns and network time persistence are two very different measures. Thus, our results reveal a new aspect of individual brain-print of functional brain networks.

In summary, the present work demonstrates that (1) the functional brain network is time persistent at network level; (2) network time persistence varies across different functional networks; and (3) individuals have characteristic network time persistence with a genetic component and can be linked to behavioral performance.

Data Availability

The datasets used in the present study are publicly available.

References

Abrol A, Damaraju E, Miller RL, Stephen JM, Claus ED, Mayer AR, Calhoun VD (2017) Replicability of time-varying connectivity patterns in large resting state fMRI samples. Neuroimage 163:160–176.

Allen EA, Damaraju E, Plis SM, Erhardt EB, Eichele T, Calhoun VD (2014) Tracking whole-brain connectivity dynamics in the resting state. Cereb Cortex 24:663–676.

Arenas A, Díaz-Guilera A, Kurths J, Moreno Y, Zhou C (2008) Synchronization in complex networks. Phys Rep 469:93–153.

Axelrod V (2014) Minimizing bugs in cognitive neuroscience programming. Front Psychol 5:1435.

Axelrod V, Rees G, Bar M (2017) The default network and the combination of cognitive processes that mediate self-generated thought. Nat Hum Behav 1:896–910.

Barabási DL, Bianconi G, Bullmore E, Burgess M, Chung S, Eliassi-Rad T, George D, Kovács IA, Makse H, Nichols TE (2023) Neuroscience needs network science. J Neurosci 43:5989–5995.

Baranes L, Shimoni H, Axelrod V (2024) Demographic and heredity correlates of day-dreaming propensity: insights from the behavioral data of the Human Connectome Project Young Adult dataset. Curr Psychol 43: 28674–28684.

Barttfeld P, Uhrig L, Sitt JD, Sigman M, Jarraya B, Dehaene S (2015) Signature of consciousness in the dynamics of resting-state brain activity. Proc Natl Acad Sci U S A 112:887–892.

Bassett DS, Bullmore ET (2009) Human brain networks in health and disease. Curr Opin Neurol 22:340–347.

Bassett DS, Gazzaniga MS (2011) Understanding complexity in the human brain. Trends Cogn Sci 15:200–209.

Berezin Y, Gozolchiani A, Guez O, Havlin S (2012) Stability of climate networks with time. Sci Rep 2:1–8.
Bijsterbosch JD, Woolrich MW, Glasser MF, Robinson EC, Beckmann CF, Van Essen DC, Harrison SJ, Smith SM (2018) The relationship between spatial configuration and functional connectivity of brain regions. Elife 7:e32992.
Blautzik J, Keeser D, Berman A, Paolini M, Kirsch V, Mueller S, Coates U, Reiser M, Teipel SJ, Meindl T (2013) Long-term test-retest reliability of resting-state networks in healthy elderly subjects and patients with amnestic mild cognitive impairment. J Alzheimers Dis 34:741–754.
Buckner RL, DiNicola LM (2019) The brain's default network: updated anatomy, physiology and evolving insights. Nat Rev Neurosci 20:593–608.
Burgess GC, Kandala S, Nolan D, Laumann TO, Power JD, Adeyemo B, Harms MP, Petersen SE, Barch DM (2016) Evaluation of denoising strategies to address motion-correlated artifacts in resting-state functional magnetic resonance imaging data from the human connectome project. Brain Connect 6:669–680.
Chen B, et al. (2015) Individual variability and test-retest reliability revealed by ten repeated resting-state brain scans over one month. PLoS One 10: e0144963.
DeYoung CG, Sassenberg TA, Abend R, Allen T, Beaty R, Bellgrove M, Blain SD, Bzdok D, Chavez RS, Engel SA (2022) Reproducible between-person brain-behavior associations do not always require thousands of individuals. Preprint. Available at: https://psyarxivcom/sfnmk
Donges JF, Donner RV, Trauth MH, Marwan N, Schellnhuber H-J, Kurths J (2011) Nonlinear detection of paleoclimate-variability transitions possibly related to human evolution. Proc Natl Acad Sci U S A 108:20422–20427.
Du H-X, Liao X-H, Lin Q-X, Li G-S, Chi Y-Z, Liu X, Yang H-Z, Wang Y, Xia M-R (2015) Test–retest reliability of graph metrics in high-resolution functional connectomics: a resting-state functional MRI study. CNS Neurosci Ther 21:802–816.
Ebstein RP, Israel S, Chew SH, Zhong S, Knafo A (2010) Genetics of human social behavior. Neuron 65:831–844.
Finn ES, Shen X, Scheinost D, Rosenberg MD, Huang J, Chun MM, Papademetris X, Constable RT (2015) Functional connectome fingerprinting: identifying individuals using patterns of brain connectivity. Nat Neurosci 18:1664.
Ghosh SS, Kakunoori S, Augustinack J, Nieto-Castanon A, Kovelman I, Gaab N, Christodoulou JA, Triantafyllou C, Gabrieli JD, Fischl B (2010) Evaluating the validity of volume-based and surface-based brain image registration for developmental cognitive neuroscience studies in children 4 to 11 years of age. Neuroimage 53:85–93.
Glahn D, Winkler A, Kochunov P, Almasy L, Duggirala R, Carless MA, Curran J, Olvera R, Laird A, Smith S (2010) Genetic control over the resting brain. Proc Natl Acad Sci U S A 107:1223–1228.
Glasser MF, et al. (2013) The minimal preprocessing pipelines for the Human Connectome Project. Neuroimage 80:105–124.
Glasser MF, et al. (2016) A multi-modal parcellation of human cerebral cortex. Nature 536:171.
Gordon EM, et al. (2017) Precision functional mapping of individual human brains. Neuron 95:791–807.e7.
Gratton C, et al. (2018) Functional brain networks are dominated by stable group and individual factors, not cognitive or daily variation. Neuron 98:439–452.e5.
Griffanti L, et al. (2014) ICA-based artefact removal and accelerated fMRI acquisition for improved resting state network imaging. Neuroimage 95:232–247.
Hagler DJ, et al. (2019) Image processing and analysis methods for the Adolescent Brain Cognitive Development Study. Neuroimage 202:116091.
Harms MP, et al. (2018) Extending the Human Connectome Project across ages: imaging protocols for the lifespan development and aging projects. Neuroimage 183:972–984.
He BJ (2011) Scale-free properties of the functional magnetic resonance imaging signal during rest and task. J Neurosci 31:13786–13795.
Hodgson K, et al. (2017) Shared genetic factors influence head motion during MRI and body mass index. Cereb Cortex 27:5539–5546.
Hommes C (2021) Behavioral and experimental macroeconomics and policy analysis: a complex systems approach. J Econ Lit 59:149–219.
Hudetz AG, Liu X, Pillay S (2015) Dynamic repertoire of intrinsic brain states is reduced in propofol-induced unconsciousness. Brain Connect 5:10–22.
Hurst HE (1951) Long-term storage capacity of reservoirs. Trans Am Soc Civil Eng 116:770–799.
Hutchison RM, Womelsdorf T, Allen EA, Bandettini PA, Calhoun VD, Corbetta M, Della Penna S, Duyn JH, Glover GH, Gonzalez-Castillo J (2013) Dynamic functional connectivity: promise, issues, and interpretations. Neuroimage 80:360–378.
Janes AC, Peechatka AL, Frederick BB, Kaiser RH (2020) Dynamic functioning of transient resting-state coactivation networks in the Human Connectome Project. Hum Brain Mapp 41:373–387.
Jun S, Alderson TH, Altmann A, Sadaghiani S (2022) Dynamic trajectories of connectome state transitions are heritable. Neuroimage 256:119274.
Koscielny-Bunde E, Bunde A, Havlin S, Roman HE, Goldreich Y, Schellnhuber H-J (1998) Indication of a universal persistence law governing atmospheric variability. Phys Rev Lett 81:729.
Kriegeskorte N, Simmons WK, Bellgowan PSF, Baker CI (2009) Circular analysis in systems neuroscience: the dangers of double dipping. Nat Neurosci 12:535–540.
Kringelbach ML, Deco G (2020) Brain states and transitions: insights from computational neuroscience. Cell Rep 32:108128.
Laumann TO, et al. (2017) On the stability of BOLD fMRI correlations. Cereb Cortex 27:4719–4732.
Laumann TO, Snyder AZ, Gratton C (2024) Challenges in the measurement and interpretation of dynamic functional connectivity. Imaging Neurosci 2:1–19.
Lee HJ, Dworetsky A, Labora N, Gratton C (2025) Using precision approaches to improve brain-behavior prediction. Trends Cogn Sci 29: 170–183.
Leonardi N, Van De Ville D (2015) On spurious and real fluctuations of dynamic functional connectivity during rest. Neuroimage 104:430–436.
Levman J, MacDonald P, Lim AR, Forgeron C, Takahashi E (2017) A pediatric structural MRI analysis of healthy brain development from newborns to young adults. Hum Brain Mapp 38:5931–5942.
Li J, Kong R, Liégeois R, Orban C, Tan Y, Sun N, Holmes AJ, Sabuncu MR, Ge T, Yeo BT (2019) Global signal regression strengthens association between resting-state functional connectivity and behavior. Neuroimage 196:126–141.
Linkenkaer-Hansen K, Nikouline VV, Palva JM, Ilmoniemi RJ (2001) Long-range temporal correlations and scaling behavior in human brain oscillations. J Neurosci 21:1370–1377.
Liu J, Liao X, Xia M, He Y (2018) Chronnectome fingerprinting: identifying individuals and predicting higher cognitive functions using dynamic brain connectivity patterns. Hum Brain Mapp 39:902–915.
Ludescher J, Gozolchiani A, Bogachev MI, Bunde A, Havlin S, Schellnhuber HJ (2013) Improved El Niño forecasting by cooperativity detection. Proc Natl Acad Sci U S A 110:11742–11745.
Lurie DJ, Kessler D, Bassett DS, Betzel RF, Breakspear M, Keilholz S, Kucyi A, Liégeois R, Lindquist MA, McIntosh AR (2019) Questions and controversies in the study of time-varying functional connectivity in resting fMRI. Netw Neurosci 4:30–69.
Ma Z, Zhang N (2018) Temporal transitions of spontaneous brain activity. Elife 7:e33562.
Makowski C, Brown TT, Zhao W, Hagler DJ, Parekh P, Garavan H, Nichols TE, Jernigan TL, Dale AM (2023) Reports of the death of brain-behavior associations have been greatly exaggerated. Preprint. Available at: https://wwwbiorxivorg/content/101101/20230616545340v1abstract:2023.2006.2016.545340
Marek S, et al. (2022) Reproducible brain-wide association studies require thousands of individuals. Nature 603:654–660.
Markov NT, Ercsey-Ravasz M, Van Essen DC, Knoblauch K, Toroczkai Z, Kennedy H (2013) Cortical high-density counterstream architectures. Science 342:1238406.
Mashour GA, Roelfsema P, Changeux J-P, Dehaene S (2020) Conscious processing and the global neuronal workspace hypothesis. Neuron 105:776–798.
Mizrahi T, Axelrod V (2023) Naturalistic auditory stimuli with fNIRS prefrontal cortex imaging: a potential paradigm for disorder of consciousness diagnostics (a study with healthy participants). Neuropsychologia 187: 108604.
Noble S, Scheinost D, Constable RT (2019) A decade of test-retest reliability of functional connectivity: a systematic review and meta-analysis. Neuroimage 203:116157.
Northoff G, Lamme V (2020) Neural signs and mechanisms of consciousness: is there a potential convergence of theories of consciousness in sight? Neurosci Biobehav Rev 118:568–587.
Palva JM, Zhigalov A, Hirvonen J, Korhonen O, Linkenkaer-Hansen K, Palva S (2013) Neuronal long-range temporal correlations and avalanche

dynamics are correlated with behavioral scaling laws. Proc Natl Acad Sci U S A 110:3585–3590.
Peng C-K, Buldyrev SV, Havlin S, Simons M, Stanley HE, Goldberger AL (1994) Mosaic organization of DNA nucleotides. Phys Rev E 49:1685.
Power JD, Barnes KA, Snyder AZ, Schlaggar BL, Petersen SE (2012) Spurious but systematic correlations in functional connectivity MRI networks arise from subject motion. Neuroimage 59:2142–2154.
Power JD, Cohen AL, Nelson SM, Wig GS, Barnes KA, Church JA, Vogel AC, Laumann TO, Miezin FM, Schlaggar BL (2011) Functional network organization of the human brain. Neuron 72:665–678.
Salcedo-Sanz S, Casillas-Pérez D, Del Ser J, Casanova-Mateo C, Cuadra L, Piles M, Camps-Valls G (2022) Persistence in complex systems. Phys Rep 957:1–73.
Schaefer A, Kong R, Gordon EM, Laumann TO, Zuo X-N, Holmes AJ, Eickhoff SB, Yeo BT (2018) Local-global parcellation of the human cerebral cortex from intrinsic functional connectivity MRI. Cereb Cortex 28: 3095–3114.
Shappell H, Caffo BS, Pekar JJ, Lindquist MA (2019) Improved state change estimation in dynamic functional connectivity using hidden semi-Markov models. Neuroimage 191:243–257.
Shirer WR, Jiang H, Price CM, Ng B, Greicius MD (2015) Optimization of rs-fMRI pre-processing for enhanced signal-noise separation, test-retest reliability, and group discrimination. Neuroimage 117:67–79.
Siegel JS, Mitra A, Laumann TO, Seitzman BA, Raichle M, Corbetta M, Snyder AZ (2017) Data quality influences observed links between functional connectivity and behavior. Cereb Cortex 27:4492–4502.
Smith SM, Nichols TE, Vidaurre D, Winkler AM, Behrens TE, Glasser MF, Ugurbil K, Barch DM, Van Essen DC, Miller KL (2015) A positive-negative mode of population covariation links brain connectivity, demographics and behavior. Nat Neurosci 18:1565.
Spisak T, Bingel U, Wager TD (2023) Multivariate BWAS can be replicable with moderate sample sizes. Nature 615:E4–E7.
Sporns O, Chialvo DR, Kaiser M, Hilgetag CC (2004) Organization, development and function of complex brain networks. Trends Cogn Sci 8:418–425.
Termenon M, Jaillard A, Delon-Martin C, Achard S (2016) Reliability of graph analysis of resting state fMRI using test-retest dataset from the Human Connectome Project. Neuroimage 142:172–187.
Van Essen DC, et al. (2012) The Human Connectome Project: a data acquisition perspective. Neuroimage 62:2222–2231.
Vidaurre D, Smith SM, Woolrich MW (2017) Brain network dynamics are hierarchically organized in time. Proc Natl Acad Sci U S A 114:12827–12832.
Wang Y, Gozolchiani A, Ashkenazy Y, Berezin Y, Guez O, Havlin S (2013) Dominant imprint of Rossby waves in the climate network. Phys Rev Lett 111:138501.
Wilcox RR (2012) *Introduction to robust estimation and hypothesis testing*. Amsterdam; Boston, MA: Academic Press.
Wisner KM, Atluri G, Lim KO, MacDonald AW 3rd (2013) Neurometrics of intrinsic connectivity networks at rest using fMRI: retest reliability and cross-validation using a meta-level method. Neuroimage 76:236–251.
Wu T, Gao X, An F, Sun X, An H, Su Z, Gupta S, Gao J, Kurths J (2024) Predicting multiple observations in complex systems through low-dimensional embeddings. Nat Commun 15:2242.
Yeo BT, et al. (2011) The organization of the human cerebral cortex estimated by intrinsic functional connectivity. J Neurophysiol 106:1125–1165.
Zalesky A, Fornito A, Cocchi L, Gollo LL, Breakspear M (2014) Time-resolved resting-state brain networks. Proc Natl Acad Sci U S A 111:10341–10346.
Zuo X-N, Di Martino A, Kelly C, Shehzad ZE, Gee DG, Klein DF, Castellanos FX, Biswal BB, Milham MP (2010) The oscillating brain: complex and reliable. Neuroimage 49:1432–1445.
Zuo X-N, Xing X-X (2014) Test-retest reliabilities of resting-state FMRI measurements in human brain functional connectomics: a systems neuroscience perspective. Neurosci Biobehav Rev 45:100–118.